IOP Publishing Nanotechnology
Nanotechnology **25** (2014) 235202 (6pp) doi:10.1088/0957-4484/25/23/235202

Spin-polarized currents generated by magnetic Fe atomic chains

Zheng-Zhe Lin[1] **and Xi Chen**[2]

[1] School of Physics and Optoelectronic Engineering, Xidian University, Xi'an 710071, People's Republic of China
[2] Department of Applied Physics, School of Science, Xi'an Jiaotong University, Xi'an 710049, People's Republic of China

E-mail: linzhengzhe@hotmail.com

Received 21 January 2014, revised 2 April 2014
Accepted for publication 16 April 2014
Published 21 May 2014

Abstract

Fe-based devices are widely used in spintronics because of high spin-polarization and magnetism. In this work, freestanding Fe atomic chains, the thinnest wires, were used to generate spin-polarized currents due to the spin-polarized energy bands. By *ab initio* calculations, the zigzag structure was found to be more stable than the wide-angle zigzag structure and had a higher ratio of spin-up and spin-down currents. By our theoretical prediction, Fe atomic chains have a sufficiently long thermal lifetime only at $T \leqslant 150$ K, while C atomic chains are very stable even at $T = 1000$ K. This means that the spintronic devices based on Fe chains could work only at low temperatures. A system constructed by a short Fe chain sandwiched between two graphene electrodes could be used as a spin-polarized current generator, while a C chain could not be used in this way. The present work may be instructive and meaningful to further practical applications based on recent technical developments on the preparation of metal atomic chains (*Proc. Natl. Acad. Sci. USA* **107** 9055 (2010)).

Keywords: spin-polarized current, atomic chain, quantum electron transport

(Some figures may appear in colour only in the online journal)

1. Introduction

Spintronics is a promising field for information processing, storage, and many other applications. In the past decade, much effort has been made in spintronics, and great developments have been seen [1–3]. In this area, generation and manipulation of spin-polarized current are two basic points, and minimization of spintronic devices is increasingly important. Since the discovery of graphene, more and more applications based on it have been proposed. Due to the half-metallic nature for edge states in zigzag graphene nanoribbons [4, 5]—that is, metallic for electrons with one spin orientation and insulating for electrons with the other—graphene-based spin-filter devices were proposed. However, the edges of graphene suffer from spontaneous reconstruction [6, 7] or chemical passivation, which may change the half-metallic electronic property. On the other hand, as the thinnest molecular wires, one-dimensional atomic chains have gained great attention for their possible spintronic applications. Over the past two decades, Au [8–11] and Pt [12, 13] atomic chains were prepared by pulling two contacted atom-sized metal junctions. In recent years, freestanding C chains were carved out from single-layer graphene with a high-energy electron beam [14], unraveled from sharp C specimens [15–17] or C nanotubes [18], and chemically synthesized [19–21]. Recently, much attention has been paid to metal atomic chains, and their stability has been studied [22, 23]. By elongating a C nanotube with an Fe nanorod inside, an Fe atomic chain clamped by a C nanotube was prepared [24], and the chemical reactivity and sensitivity of Au and Ag chains to small molecules were considered [25–27]. Among these atomic chains, magnetic chains may be the thinnest material used for generating and transporting spin-polarized currents because of high spin-polarization and magnetism—that is, Fe atomic chains [28]. In recent years, two-dimensional graphene was considered a good candidate for materials used in emerging electronics. In C-based circuits, one-dimensional C chains are the thinnest natural wires, and an Fe

chain embedded in a C chain may work with the circuits. C chains have been proven effective as spin-filters and spin-valves [29, 30], and a magnetic Fe chain embedded in a C chain should perform well on spin-polarized current generation. To design Fe-based low-dimensional spintronic devices, theoretical investigation on the thermal stability and electronic property of Fe chains should be beneficial to guild corresponding experiments.

In this work, the spintronic property of Fe atomic chains was studied. On this basis, a short Fe atomic chain clamped by graphene electrodes with C chains (figure 3(a)) was proposed as a spin-polarized current generator. To investigate the thermal stability of Fe atomic chains, a recently built statistical mechanical model [31–34] was employed. According to the result, the C-C and C-Fe bonds in atomic chains are very stable at room temperature, while Fe-Fe bonds could survive only below 150 K with a lifetime longer than 99 h. A designed structure composed by graphene electrodes, C chains, and an Fe chain presented a feature of spin-polarized quantum electronic transport. The structure could be used as the smallest and thinnest spin-polarized current generator possible.

2. Method

To investigate the electronic properties of Fe atomic chains and corresponding structures, density functional theory calculations were performed using the SIESTA code [35]. The exchange-correlation functional was treated using a generalized gradient approximation according to Perdew-Burke-Ernzerhof [36]. The norm-conserving Troullier-Martins pseudopotentials [37] were used to describe the core electrons. For structure optimization, the double-ζ plus polarization basis sets were used, and the grid mesh cutoff was set at 150 Ry. The structures were relaxed until the atomic forces became less than 0.01 eV Å^{-1}. For molecular dynamics (MD) simulations, a non-self-consistent Harris functional was used to save computation time.

For quantum transport, calculations were performed using the TRANSIESTA module [38]. For a bias voltage V_b, the spin-up part I_+ and spin-down part I_- of the current is given by the Landauer-Buttiker formula [39]:

$$I_{\pm} = \frac{2e}{h}\int T_{\pm}(E, V_b)\left[f_L\left(E - E_F - \frac{eV_b}{2}\right) - f_R\left(E - E_F + \frac{eV_b}{2}\right)\right]dE. \quad (1)$$

Here, $T_+(E,V_b)$ and $T_-(E,V_b)$ are the transmission rates of spin-up and spin-down electrons at energy E, respectively. E_F is the Fermi energy of the electrodes. f_L and f_R are the Fermi–Dirac distribution functions for both electrodes, respectively. To save computation time, the single-ζ plus polarization basis sets were used.

A simple statistical mechanical model [31–34] built previously was applied to predict the lifetime of chemical bonds in atomic chains at different temperatures. In atomic chains, an element process may involve a transfer of a 'key atom' in a potential valley crossing over E_0. In most cases, the atomic kinetic energy ε at the valley bottom is significantly smaller than E_0, and the atom vibrates many times in the valley before crossing over the barrier. Based on the Boltzmann distribution, the probability P of the atomic kinetic energy ε larger than E_0 reads:

$$P = \frac{\int_{E_0}^{+\infty}\varepsilon^{1/2}e^{-\varepsilon/k_BT}d\varepsilon}{\int_{0}^{+\infty}\varepsilon^{1/2}e^{-\varepsilon/k_BT}d\varepsilon} = \frac{\int_{E_0}^{+\infty}\varepsilon^{1/2}e^{-\varepsilon/k_BT}d\varepsilon}{\sqrt{\pi}\left(k_BT\right)^{3/2}/2}, \quad (2)$$

where $\varepsilon^{1/2}e^{-\varepsilon/k_BT}$ is the Boltzmann distribution and $\int_0^{+\infty}\varepsilon^{1/2}e^{-\varepsilon/k_BT}d\varepsilon$ is the partition function. Then, the atomic transfer rate k_{1st} over the barrier reads:

$$k_{1st} = k_0\frac{\int_{E_0}^{+\infty}\varepsilon^{1/2}e^{-\varepsilon/k_BT}d\varepsilon}{\sqrt{\pi}\left(k_BT\right)^{3/2}/2}, \quad (3)$$

and the thermal lifetime of the chemical bond is $\tau = 1/k_{1st}$. Here, k_0 is the attempt frequency of the key atom vibrating in the potential valley, which can be evaluated by the potential energy $U = U(s)$ along the reaction path with $ds = \left(\sum_{i=1}^{n} m_i d\vec{r}_i^{\,2}\right)^{1/2}$ as the reaction coordinate. The Lagrangian along the reaction path is:

$$L = \frac{1}{2}\left(\frac{ds}{dt}\right)^2 - U, \quad (4)$$

and the corresponding Lagrange's equation approximately reads:

$$\frac{d^2s}{dt^2} + k_0^2 s = 0, \quad (5)$$

where $k_0 = \left.\frac{d^2U}{ds^2}\right|_{s=0}$ is just the attempt frequency. In our previous work, this model was widely verified by reaction rate data from MD simulations [31–34].

3. Results and discussion

3.1. General information of infinite Fe atomic chains

To get basic information, geometry optimizations and energy band calculations were performed for infinite Fe atomic chains. Linear and zigzag Fe chains were taken into account as possible structures, and considering the Peierls distortion, a unit cell with two atoms was used. According to the result, the zigzag structure (upper figure 1(a)) has the lowest potential energy, and with the Peierls distortion, the corresponding bond lengths are $c_1 = 2.37$ Å, $c_2 = 2.55$ Å, and $c = 2.62$ Å. The cohesive energy and the magnetic moment per unit cell are $E_c = 2.64$ eV/atom and $\mu = 3.80\,\mu_B$, respectively. The above result is close to reference [40] ($c_1 = 2.24$ Å, $c_2 = 2.42$ Å, $c = 2.40$ Å, $E_c = 2.69$ eV/atom, and $\mu = 3.19\,\mu_B$, by ultrasoft pseudopotentials and the plane-wave basic set). It is worth

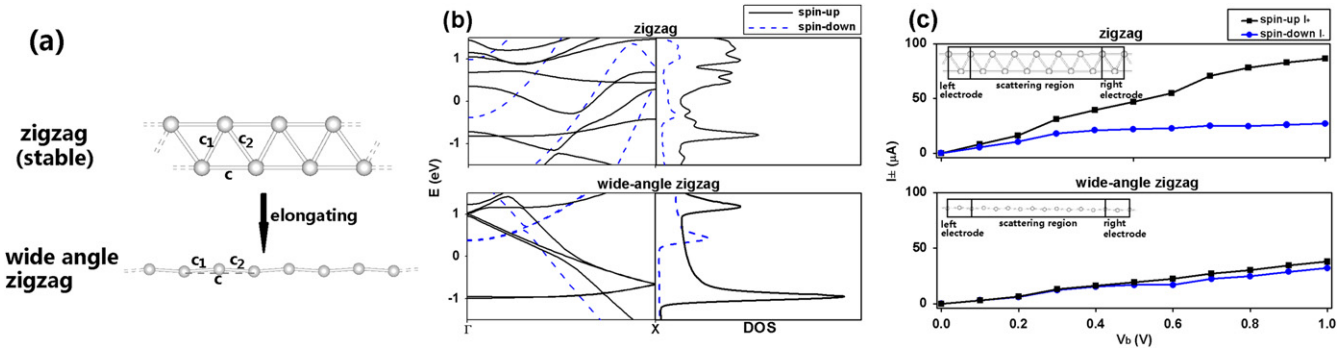

Figure 1. (a) The zigzag structure of an infinite Fe atomic chain (upper) and the wide-angle zigzag structure (lower) that is elongated from the zigzag one. (b) The energy bands and DOS of zigzag (upper) and wide-angle zigzag (lower) Fe atomic chains, where Γ is the center and X is the boundary of the Brillouin zone. (c) The spin-up and spin-down current I_+ and I_- at different bias V_b for zigzag (upper) and wide-angle zigzag (lower) Fe atomic chains.

noting that in some papers the Fe chain was simply considered as a linear atomic chain [28, 41, 42], which may be not the most stable structure. Figure 1(b) (upper) shows the energy band profile and the density of state (DOS) for the zigzag Fe atomic chain, presenting a spin-polarized feature. To investigate the quantum transport property, a model was built by one and six unit cells of a zigzag Fe chain selected as the electrode and the scattering region, respectively (figure 1(c)). A $1\times1\times100$ k-point sampling was used for the electrodes, and a vacuum layer of 20 Å was used along x and y directions to minimize the interaction between neighboring unit cells. The result (upper figure 1(c)) indicates that the current is spin-polarized and I_+: $I_-=3.2$ at $V_b=1.0$ V. In the range of $V_b=0.0\sim1.0$ V, the average conductances for spin-up and spin-down electrons are about 1.11 and 0.35 G_0 ($G_0=2e^2/h$ is the quantum conductance), respectively, which is close to the values in reference [43].

In an experimental manipulation of nanostructures such as mechanically controllable break junctions [8–13], an atomic chain can be elongated. To investigate the effect of elongation on an Fe chain, we enlarged the lattice constant c of a zigzag Fe chain step by step and performed geometry optimizations. According to the result, another local minima of potential energy was found at $c=4.68$ Å, which is elongated from a zigzag Fe chain and can be called a wide-angle zigzag Fe chain (lower figure 1(a)). This stable structure has a smaller cohesive energy $E_c=1.77$ eV/atom than the zigzag structure and a magnetic moment $\mu=3.57$ μ_B per unit cell. Figure 1(b) (lower) shows the energy band profile and DOS of the wide-angle zigzag Fe atomic chain, presenting a spin-polarized feature. For quantum transport, the current is less spin-polarized than that of the zigzag chain (lower figure 1(c)), with a ratio of I_+: $I_-=1.2$ at $V_b=1.0$ V. In the range of $V_b=0.0\sim1.0$ V, the average conductances for spin-up and spin-down electrons are about 0.49 and 0.42 G_0, respectively.

3.2. Thermal lifetime of C_8, C_4FeC_4, and $C_4Fe_4C_4$ chains

The stability of Fe atomic chains is vitally important in practical applications and must be investigated. Recently, a theoretical model was proposed to formulate criteria for the producibility of freestanding metal atomic chains in mechanically controllable break junctions [22], and the producibility of C atomic chains was also studied [44, 45]. Here, we consider the thermal lifetime of Fe chains connected with C chains—that is, C_8, C_4FeC_4, and $C_4Fe_4C_4$ chains (figure 2(a)). In thermal motion, a chemical bond in the chain may break when two neighboring atoms move away from each other (e.g., the progress shown in figure 2(a)), and the average lifetime of the bond is $\tau=1/k_{1st}$, where k_{1st} can be evaluated by equations (3) and (5). To apply equations (3) and (5), the potential profiles along the minimum energy paths (MEPs) for bond breaking of the C-C in the C_8 chain, the C-Fe in the C_4FeC_4 chain, and the middle Fe-Fe in the $C_4Fe_4C_4$ chain (figure 2(b)) were calculated with two terminal chain atoms fixed. As an example, the MEP for bond breaking of the middle Fe-Fe bond in the $C_4Fe_4C_4$ chain is shown in figure 1(a). For the above bond-breaking processes, we got $E_0=5.44$, 5.17, and 0.51 eV and $k_0=8.05\times10^{11}$, 1.93×10^{11}, and 5.75×10^{10} s^{-1} (by equation (5)), respectively. Then, by equation (3), the average lifetime τ of the bonds at different temperatures was derived (figure 2(c)). According to equations (3) and (5), the middle C-C bond in the C_8 chain has a lifetime of about 6×10^{70} years at $T=300$ K. Even at $T=1000$ K, this bond still has a lifetime of about 1×10^7 years. For the C-Fe bond in the C_4FeC_4 chain, the lifetime is about 6×10^{66} and 2×10^6 years at $T=300$ and 1000 K, respectively. The result indicates that the pure and Fe-doped C chains are very stable. However, at $T=300$ K, the middle Fe-Fe bond in the $C_4Fe_4C_4$ chain has a lifetime of only 1.30 ms. Fortunately, at $T\leqslant150$ K, the lifetime is predicted to be longer than 99 h. By *ab initio* MD simulation, we found that at $T=300$ K, the middle Fe-Fe bond of the $C_4Fe_4C_4$ chain kept stable even in a time of 50 ps, while it survived for only 0.2 ps at $T=1000$ K. This result is generally in accordance with the above theoretical prediction. For this reason, Fe atomic chains may serve as spintronic devices at low temperatures.

3.3. Spin-polarized electronic transport

Based on optimized structures, we investigated the spintronic properties of an Fe atomic chain coupled with a C chain, which is the thinnest magnetic wire in a graphene-based

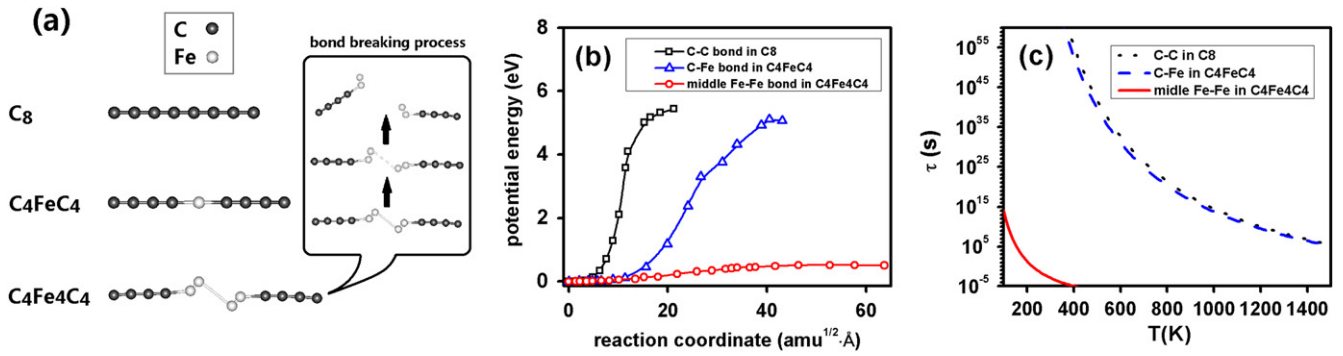

Figure 2. (a) The structures of C_8, C_4FeC_4, and $C_4Fe_4C_4$ atomic chains. The right panel shows some snapshots along the MEP for bond breaking of the middle Fe-Fe bond. (b) Potential energy profile along the MEP for bond breaking of C-C in the C_8 chain, C-Fe in the C_4FeC_4 chain, and middle Fe-Fe in the $C_4Fe_4C_4$ chain. (c) The average lifetime $\tau = 1/k_{1st}$ of these three bonds changing with temperature T.

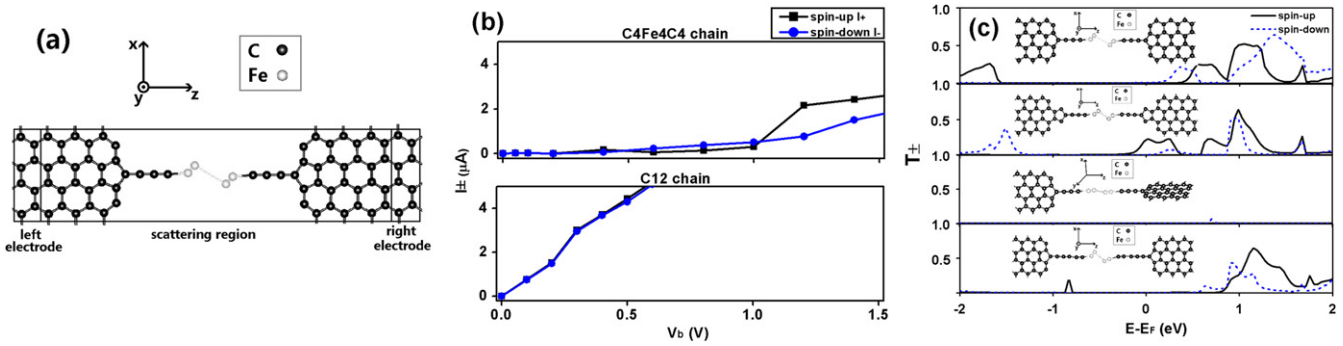

Figure 3. (a) A two-probe system constructed by a $C_4Fe_4C_4$ atomic chain as the scattering region sandwiched between two semi-infinite graphene electrodes. Periodic boundary conditions are shown by the solid frame. (b) The spin-up and spin-down current I_+ and I_- at a different bias V_b for a $C_4Fe_4C_4$ (upper) chain and a C_{12} (lower) chain sandwiched between graphene electrodes. (c) Transmission spectra at $V_b = 0$ V for four two-probe systems including a C-Fe-C atomic chain. Corresponding scattering regions are shown in each subfigure. The solid and dashed lines indicate T_+ and T_- for spin-up and spin-down electrons, respectively.

circuit. A two-probe system, with a $C_4Fe_4C_4$ atomic chain as the scattering region sandwiched between two semi-infinite graphene electrodes, was constructed along the z direction (figure 3(a)). Periodic boundary conditions are imposed on the electrodes (on the x and z directions) and the scattering region (on the x direction), as shown by the solid frame. Different lengths of buffer layers in the scattering region were tested to investigate the influence between the two electrodes, and three unit cells of the electrode were found to be enough. The zigzag direction of graphene electrodes was chosen as the z direction, because the k vectors of the electronic states near the Fermi energy—that is, on the Dirac point—are along the z direction, and thus the conductivity of the zigzag direction is better than the armchair direction [46]. A $4 \times 1 \times 100$ k-point sampling was used for the electrodes. The vacuum layer along the y direction is 20 Å to minimize the interaction between neighboring sheets.

According to the result (upper figure 3(b)), for $V_b = 0.6 \sim 1.0$ V, the spin-down current I_- is larger than the spin-up current I, presenting a spin-polarized feature. The ratio is I_-: $I_+ = 3.8$ at $V_b = 0.6$ V, and it decreases to I_-: $I_+ = 1.7$ at $V_b = 1.0$ V. However, in this voltage range the current is quite small, and the average conductances for spin-up and spin-down electrons are only 0.008 and 0.009 G_0, respectively. For $V_b > 1.0$ V, the current is larger than that for $V_b = 0.6 \sim 1.0$ V, and the spin-up current I_+ is obviously larger than the spin-down current I_-. At $V_b = 1.4$ V, the ratio I_+: $I_- = 1.6$. By comparison, at the same V_b, I_+ and I_- of this system are in an order of magnitude smaller than those of an infinite Fe atomic chain. In the range of $V_b = 1.0 \sim 1.4$ V, the average conductances for spin-up and spin-down electrons are about 0.05 and 0.03 G_0, respectively. To investigate the mechanism of spin-polarized currents, the transmission spectrum at $V_b = 0$ V for the two-probe system in figure 3(a) is plotted in the first subfigure of figure 3(c). Transmission peaks for spin-up and spin-down electrons can be found at different energy E. These peaks should correspond to molecular electronic states of the scattering region. In the range of E-$E_F = 0 \sim 1$ eV, a spin-down transmission peak locates at an energy range lower than a spin-up peak. Therefore, with increasing V_b, the spin-down current I_- is first larger and then smaller than the spin-up current I_+. In the range of E-$E_F > 1$ eV, another spin-up transmission peak appears with higher transmission than the spin-down peak in this range, and correspondingly for $V_b > 1.0$ V, I_+ is larger than I_-.

To investigate the influence of different shapes of electrode ends or lengths of a C chain on the spin-polarized currents, three other structures (shown in the second to fourth subfigures of figure 3(c)) were considered, which consist of

the one with tapered electrode ends, the one whose electrode planes are perpendicular to each other, and the one with longer C chains, respectively. For the structure with tapered electrode ends, the transmission of spin-up electrons is always larger than spin-down electrons in the range of $E\text{-}E_F = 0 \sim 2$ eV, indicating that the currents are spin-polarized. For the structure whose electrode planes are perpendicular to each other, the transmission of spin-up and spin-down electrons is nearly zero in the whole energy range—that is, the conductance is very low at any V_b. This is because in this case the $p\text{-}\pi$ conjugated orbitals in graphene electrodes are orthogonal to each side and then the transmission is forbidden. It can be inferred that when the two electrodes have an angle θ, the transmission $T_{\pm}$ is proportional to $\cos^2\theta$. For the structure with longer C chains, the transmission of spin-up electrons is also larger than spin-down electrons in the range of $E\text{-}E_F > 1$ eV. In summary, for $V_b > 1$ eV, the spin-polarized currents by the Fe atomic chain are independent of the geometry of electrodes or C chains but are weakened by the increase in angle between the two electrodes.

Finally, to make a comparison with a pure C atomic chain, we replaced four Fe atoms with four C atoms, and I_+ and I_- of the optimized structure are shown in lower figure 3(b). It can be seen that the pure C chain exhibits the typical characteristics of spin-non-polarized conductors, with a conductance of about 0.11 G_0 for spin-up and spin-down electrons. According to the above results, Fe atomic wire could act as a spin-polarized current generator in C-based circuits.

4. Conclusions

Through the above theoretical investigation, freestanding Fe atomic chains were proposed to be used as the thinnest wire to generate spin-polarized currents. A long Fe chain has a stable zigzag structure and a spin-polarized energy band. At a bias of 1.0 V, the ratio of spin-up and spin-down current in a zigzag Fe chain is about 3.2:1. When a zigzag Fe chain is elongated, it transforms into a wide-angle zigzag structure, whose ratio of spin-up and spin-down current is lower than that of a zigzag structure (1.2:1 at 1.0 V). By our theoretical prediction, Fe atomic chains have sufficiently long thermal lifetimes only at $T \leqslant 150$ K, while C atomic chains are very stable even at $T = 1000$ K. This result means that the spintronic devices based on Fe chains could work only at low temperatures. A short Fe chain sandwiched between two graphene electrodes was taken as an example for spintronic devices, and the quantum electronic transport was investigated. At a certain bias, the currents through this system are spin-polarized, while a similar property was not found for pure C chains. By recently developed techniques for preparing Fe chains clamped by C nanotubes [24], the spintronic property of Fe chains may be put into future practical applications.

Acknowledgments

This work was supported by the National Natural Science Foundation of China under Grant No. 11304239, and the Fundamental Research Funds for the Central Universities.

References

[1] Wolf S, Awschalom D, Buhrman R, Daughton J, Von Molnar S, Roukes M, Chtchelkanova A and Treger D 2001 *Science* **294** 1488
[2] Zutic I, Fabian J and Das Sarma S 2004 *Rev. Mod. Phys.* **76** 323
[3] Fert A 2008 *Rev. Mod. Phys.* **80** 1517
[4] Son Y-W, Cohen M L and Louie S G 2006 *Nature* **444** 347
[5] Saffarzadeh A and Farghadan R 2011 *Appl. Phys. Lett.* **98** 023106
[6] Koskinen P, Malola S and Häkkinen H 2009 *Phys. Rev.* B **80** 073401
[7] Koskinen P, Malola S and Häkkinen H 2008 *Phys. Rev. Lett.* **101** 115502
[8] Ohnishi H, Kondo Y and Takayanagi K 1998 *Nature* **395** 780
[9] Yanson A I, Bollinger G R, van den Brom H E, Agraït N and van Ruitenbeek J M 1998 *Nature* **395** 783
[10] Kizuka T 1998 *Phys. Rev. Lett.* **81** 4448
[11] Rodrigues V, Fuhrer T and Ugarte D 2000 *Phys. Rev. Lett.* **85** 4124
[12] Krans J M, Muller C J, Yanson I K, Govaert T C M, Hesper R and van Ruitenbeek J M 1993 *Phys. Rev.* B **48** 14721
[13] Kizuka T and Monna K 2009 *Phys. Rev.* B **80** 205406
[14] Jin C, Lan H, Peng L, Suenaga K and Iijima S 2009 *Phys. Rev. Lett.* **102** 205501
[15] Mikhailovskij I M, Wanderka N, Ksenofontov V A, Mazilova T I, Sadanov E V and Velicodnaja O A 2007 *Nanotech.* **18** 475705
[16] Mazilova T I, Mikhailovskij I M, Ksenofontov V A and Sadanov E V 2009 *Nano Lett.* **9** 774
[17] Mikhailovskij I M, Sadanov E V, Mazilova T I and Velicodnaja O A 2009 *Phys. Rev.* B **80** 165404
[18] Börrnert F *et al* 2010 *Phys. Rev.* B **81** 085439
[19] Eisler S, Slepkov A D, Elliott E, Luu T, McDonald R, Hegmann F A and Tykwinski R R 2005 *J. Am. Chem. Soc.* **127** 2666
[20] Chalifoux W A, McDonald R, Ferguson M J and Tykwinski R R 2009 *Angew. Chem. Int. Edit.* **48** 7915
[21] Chalifoux W A and Tykwinski R R 2010 *Nat. Chem.* **2** 967
[22] Thiess A, Mokrousov Y, Blügel S and Heinze S 2008 *Nano Lett.* **8** 2144
[23] Zaki N, Marianetti C A, Acharya D P, Zahl P, Sutter P, Okamoto J, Johnson P D, Millis A J and Osgood R M 2013 *Phys. Rev.* B **87** 161406(R)
[24] Tang D-M, Yin L-C, Li F, Liu C, Yu W-J, Hou P-X, Wu B, Lee Y-H, Ma X-L and Cheng H-M 2010 *Proc. Natl. Acad. Sci. USA* **107** 9055
[25] Ishida H 2007 *Phys. Rev.* B **75** 205419
[26] Sclauzero G, Dal Corso A and Smogunov A 2012 *Phys. Rev.* B **85** 165411
[27] Sclauzero G and Corso A D 2013 *Phys. Rev.* B **87** 085108
[28] Dalgleish H and Kirczenow G 2005 *Phys. Rev.* B **72** 155429
[29] Zeng M G, Shen L, Cai Y Q, Sha Z D and Feng Y P 2010 *Appl. Phys. Lett.* **96** 042104
[30] Xu Y, Wang B-J, Ke S-H, Yang W and Alzahrani A Z 2012 *J. Chem. Phys.* **137** 104107
[31] Lin Z-Z and Ning X J 2011 *EPL* **95** 47012
[32] Lin Z-Z and Chen X 2013 *EPL* **101** 48002
[33] Yu W-F, Lin Z-Z and Ning X-J 2013 *Phys. Rev.* E **87** 062311
[34] Yu W-F, Lin Z-Z and Ning X-J 2013 *Chin. Phys.* B **22** 116802

[35] Soler J M, Artacho E, Gale J D, García A, Junquera J, Ordejón P and Sánchez-Portal D 2002 *J. Phys.: Condens. Matter* **14** 2745
[36] Perdew J P, Burke K and Ernzerhof M 1996 *Phys. Rev. Lett.* **77** 3865
[37] Troullier N and Martins J L 1991 *Phys. Rev.* B **43** 1993
[38] Brandbyge M, Mozos J L, Ordejón P, Taylor J and Stokbro K 2002 *Phys. Rev.* B **65** 165401
[39] Büttiker M, Imry Y, Landauer R and Pinhas S 1985 *Phys. Rev.* B **31** 6207
[40] Ataca C, Cahangirov S, Durgun E, Jang Y-R and Ciraci S 2008 *Phys. Rev.* B **77** 214413
[41] Smogunov A, Dal Corso A and Tosatti E 2004 *Phys. Rev.* B **70** 045417
[42] Autès G, Barreteau C, Spanjaard D and Desjonquères M-C 2008 *Phys. Rev.* B **77** 155437
[43] Velev J and Butler W H 2004 *Phys. Rev.* B **69** 094425
[44] Wang Y, Ning X-J, Lin Z-Z, Li P and Zhuang J 2007 *Phys. Rev.* B **76** 165423
[45] Wang Y, Lin Z-Z, Zhang W, Zhuang J and Ning X-J 2009 *Phys. Rev.* B **80** 233403
[46] Shen L, Zeng M G, Yang S-W, Zhang C, Wang X and Feng Y P 2010 *J. Am. Chem. Soc.* **132** 11481